Sulfonated Poly(arylene ether sulfone ketone) Multiblock Copolymers with Highly Sulfonated Block. Fuel Cell Performance

Byungchan Bae,[†] Takeshi Yoda,[‡] Kenji Miyatake,*[,†,‡] Makoto Uchida,[†] Hiroyuki Uchida,[†,‡] and Masahiro Watanabe*[,†]

Fuel Cell Nanomaterials Center and Clean Energy Research Center, University of Yamanashi, 4 Takeda, Kofu 400-8510, Japan

Received: June 9, 2010; Revised Manuscript Received: July 5, 2010

Poly(arylene ether sulfone ketone) (SPESK) multiblock copolymers having highly sulfonated hydrophilic blocks were synthesized and the fuel cell performance with the copolymers was investigated. A membrane electrode assembly (MEA) using an SPESK ionomer with an ion exchange capacity of 1.8 mequiv g^{-1} as membrane and Nafion as the electrode binder showed comparable fuel cell performance and ohmic resistance to that using a Nafion NRE 211 membrane at 80 °C and 30% relative humidity (RH). A Nafion-free, all-SPESK MEA using SPESK as both the membrane and the binder was operable at 100 °C and 50% RH. The fuel cell performance was limited not only by the proton conductivity of the SPESK membrane but also by the low water flux through the membrane and specific adsorption of the ionomer on the platinum catalyst.

Introduction

The polymer electrolyte membrane fuel cell (PEMFC) has been researched intensively as an alternative source of clean energy since it does not release any pollutants such as carbon dioxide. The electrochemical reaction of hydrogen and oxygen produces electricity at high efficiency and pure water as the only byproduct. The electrochemical reaction takes places in the membrane-electrode-assembly (MEA), which is composed of a proton exchange membrane (PEM) sandwiched by two sets of gas diffusion electrodes (GDEs). Among a number of factors, the rate of the oxygen reduction reaction (ORR) at the cathode and the proton conductivity of the PEM are crucial in determining the PEMFC performance.

Perfluorosulfonic acid (PFSA) polymers, such as Nafion of Du Pont, are state-of-the-art materials as PEMs. The PFSA is composed of a perfluorocarbon polymer backbone with pendant perfluorosulfonic acid groups. The perfluorinated structure provides robust chemical and physical stability as well as excellent proton conductivity. However, the high production cost and environmental incompatibility remain issues for the perfluorinated materials. Acid-functionalized aromatic polymers have been studied as alternative PEMs, which include sulfonated poly(arylene ether sulfone)s (SPE),[1−3] poly(arylene ether ether ketone)s (SPEEK),[4−7] polyimides (SPI),[8,9] poly(arylene ether nitrile)s,[10] polybenzimidazoles (PBIs),[11,12] and polyphenylenes (SPP).[13−15] While some of these ionomer membranes have claimed to show high proton conductivity in the fully hydrated state, conductivity drops significantly in lower hydrated states (or under low-humidity conditions) in most cases. It is desirable that the PEM retains high conductivity at low humidity to minimize the balance of plant (BOP) and improve the total PEMFC performance especially for electric vehicle applications without the need for extra humidification systems.[16]

Recently, effective strategies have been proposed for improving the proton conductivity of aromatic ionomer membranes at low humidity. These include the block copolymer architecture and the incorporation of highly sulfonated moieties.[17−19] We have reported that an SPE with high ion exchange capacity (IEC), 3.26 mequiv g^{-1}, showed a higher proton conductivity than that of Nafion 112 at 120 °C and 20% relative humidity (RH).[17] Roy et al. reported that partially fluorinated multiblock SPE copolymers have comparable proton conductivity to that of Nafion 112 at 80 °C and 30% RH.[18] The introduction of highly sulfonated hexaphenylbenzene (sulfonic acid clusters) was confirmed to be effective by Matsumura et al.[19]

We synthesized a series of sulfonated multiblock poly(arylene ether sulfone)s (SPEs) with highly sulfonated hydrophilic blocks.[20] The hydrophilicity of the hydrophilic blocks increased so that the membranes showed a well-developed phase separation between hydrophobic and hydrophilic blocks. More recently, an advanced version of the multiblock copolymers, the sulfonated poly(arylene ether sulfone ketone)s (SPESKs) (Figure 1), were developed to achieve even higher proton conductivity. The membrane was operable in an H_2/air fuel cell at 100 °C and 30% RH successfully.[21] In our previous paper, details of the synthesis and physical properties of SPESKs were reported.[22] Further research on PEMFC performance of the SPESKs is presented in this contribution. The SPESKs were used as either PEMs, electrode binders, or both. Their PEMFC performance was investigated in detail and compared to that of Nafion.

Experimental Section

Materials. SPESK was synthesized as described previously.[21,22] The degree of polymerization of each block was controlled to be 30 for the hydrophobic block (X) and 8 for the hydrophilic block (Y). The IEC of SPESK X30Y8 was determined by titration to be 1.8 mequiv g^{-1}. The gas diffusion layer (GDL), 25BCH, and carbon-supported platinum catalyst, TEC10E70TPM, were purchased from SGL Carbon and Tanaka Kikinzoku Kogyo, respectively. Nafion NRE 212 and 211 membranes were purchased from Du Pont.

* To whom correspondence should be addressed. (K.M.) Tel: +81 55 220 8707. E-mail address: miyatake@yamanashi.ac.jp. (M.W.) Tel: +81 55 254 7091. E-mail: m-watanabe@yamanashi.ac.jp.
† Fuel Cell Nanomaterials Center.
‡ Clean Energy Research Center.

10.1021/jp1052908
Published on Web 07/23/2010

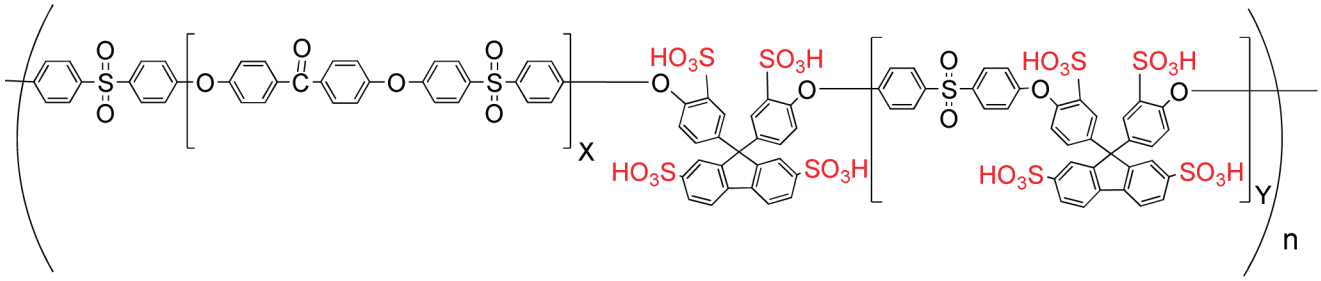

Figure 1. Chemical structure of SPESK block copolymers.

TABLE 1: Summary of MEA Constituents and Fuel Cell Test Conditions

MEA	Nafion-GDE/NRE	Nafion-GDE/SPESK	SPESK-GDE/NRE	SPESK-GDE/SPESK
cathode binder	Nafion	Nafion	SPESK	SPESK
anode binder	Nafion	Nafion	Nafion	SPESK
membrane	NRE 212, 211	SPESK	NRE 212	SPESK
(thickness)	(50, 25 μm)	(50 or 25 μm)	(50 μm)	(50 μm)
GDL	SGL25BCH (including MPL)			
Pt catalyst	0.45 mg-Pt cm^{-2} (TEC10E70TPM)			
binder/C mass ratio	0.7			
gas flow	70% utilization for anode and 40% utilization for cathode		fixed flow rate (200 mL/min for both electrodes)	
geometric area of the electrodes	29.2 cm^2		3.8 cm^2	

Preparation of Nafion-GDEs and SPESK-GDEs. Two kinds of GDE were prepared with SPESK and Nafion binders, which are denoted as SPESK-GDE and Nafion-GDE, respectively. An identical preparation procedure was applied to both GDEs, except for the dispersing solvent. The general preparation method of the Nafion-GDEs was as follows. A slurry of Pt catalyst (Pt/C, TEC10E70TPM, 68 wt %-Pt) containing Nafion binder solution (DE521) with mass ratio of Nafion/C = 0.7 was mixed in a planetary ball-mill for 30 min. The paste obtained was uniformly coated on the GDL at 60 °C by use of a pulse-swirl-spray apparatus (PSS, Nordson Co., Ltd.) followed by drying at 60 °C under vacuum. For the preparation of SPESK-GDEs, SPESK as the binder and *N*,*N*-dimethylacetamide (DMAc) as the solvent were used. The mass ratio of SPESK/C was also adjusted to 0.7, which was the same as that for the Nafion-GDE. The GDEs thus prepared were washed with hot water and 1 M nitric acid at 60 °C. The loading amount of Pt in the GDEs was 0.45 ± 0.1 mg cm^{-2}.

Preparation of Membrane Electrode Assemblies (MEAs). Two different cells were used. One was the standard test cell of the Japan Automobile Research Institute (JARI), with geometric area of 29.2 cm^2, for comparison of the MEAs with different membranes. Either a Nafion NRE membrane or an SPESK membrane was sandwiched by two Nafion-GDEs and hot-pressed at 140 °C and 1.0 MPa for 3 min to give Nafion-GDE MEAs (Nafion-GDE/NRE and Nafion-GDE/SPESK). These Nafion-GDE MEAs were tested in the JARI cell.

Another cell used in this study was an in-house designed circular test cell in which the geometric area was 3.8 cm^2, equipped with a reversible hydrogen electrode (RHE). The performance of the SPESK ionomers was tested with this circular cell not only as the cathode binder but also as a fluorine-free MEA (as both electrode binder and membrane). The former is referred to as an SPESK-GDE/NRE cell and the latter as an all-SPESK (or SPESK-GDE/SPESK) cell. The SPESK-GDE/NRE MEA was prepared by hot-pressing a Nafion NRE212 membrane sandwiched by an SPESK-GDE (as cathode) and a Nafion-GDE (as anode) at 140 °C and 1.0 MPa for 3 min. An SPESK membrane and two SPESK-GDEs were assembled to provide an all-SPESK (SPESK-GDE/SPESK) MEA without hot-pressing, which was placed into the circular cell.

Fuel Cell Test and Electrochemical Properties of MEAs. Fuel cells were operated at 80, 100, and 120 °C with various humidification levels at ambient pressure. The MEA constitution and fuel cell test conditions are summarized in Table 1. In the JARI cell, the gas utilization was controlled to be 70% for hydrogen and 40% for oxygen and air, respectively. In the circular cell, a fixed gas flow rate (200 mL min^{-1}) was used for all gases. The calculated utilizations of H_2 and air at 1 A cm^{-2} were 13 and 32%, respectively. Current−cell voltage ($I-V$) and current−cathode potential ($I-E$) curves and ohmic potential drops (IR-drop) were measured by use of a pulse generator system that included current interrupter (NCPG, Nikko Keisoku) under steady-state operation. The IR-drop was measured by applying current-off pulses for 100 μs to the cell and recording the resulting potential drop with a storage oscilloscope (VC6023, Hitachi).

For evaluating the performance of the binders, cyclic voltammograms (CVs) were measured in the circular cell by use of a potentiostat (PGST30 AUTOLAB system, ECO−CHEMIE). The test conditions were the same as those for the $I-E$ curve measurements. The cathode compartment was purged with N_2 (150 mL min^{-1}, 100% RH), while H_2 gas (100 mL min^{-1}, 100% RH) was supplied to the anode. Prior to the potential sweep, the potential was maintained at 0.08 V versus anode for 3 s. Then, the N_2 flow was stopped, and the cathode potential was swept from 0.08 to 1.00 V at a scan rate of 20 mV s^{-1}. The electrochemically active surface area (ECA) was determined from the hydrogen adsorption charge in the negative-going potential scan, referred to $\Delta Q_H^\circ = 0.21$ mC cm^{-2}, adopted conventionally for clean polycrystalline platinum.[23,24] The oxide formation charge ($Q_{Pt\ oxide}$) was calculated in the positive-going potential scan of the CV in which the double layer charge was subtracted.

Results and Discussion

Performance of Nafion-GDE/SPESK MEAs. In this study, an SPESK block copolymer with an IEC of 1.8 mequiv g^{-1} ($X = 30$, $Y = 8$) was investigated. The in-plane proton conductivity from impedance spectroscopy and water uptake data of the copolymer membrane at 80 and 110 °C are summarized in

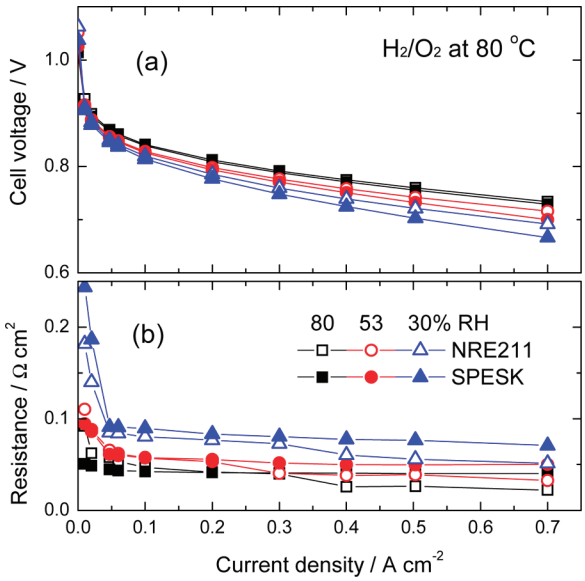

Figure 2. (a) Cell voltage and (b) ohmic resistance of H_2/O_2 fuel cells with Nafion-GDE/SPESK and Nafion-GDE/NRE 211 MEAs at 80 °C (both membranes are 25 μm thick).

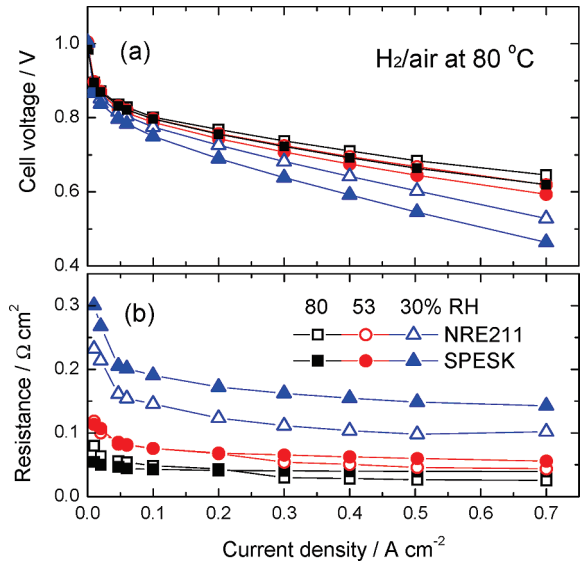

Figure 3. (a) Cell voltage and (b) ohmic resistance of H_2/air fuel cells with Nafion-GDE/SPESK and Nafion-GDE/NRE 211 MEAs at 80 °C (both membranes are 25 μm thick).

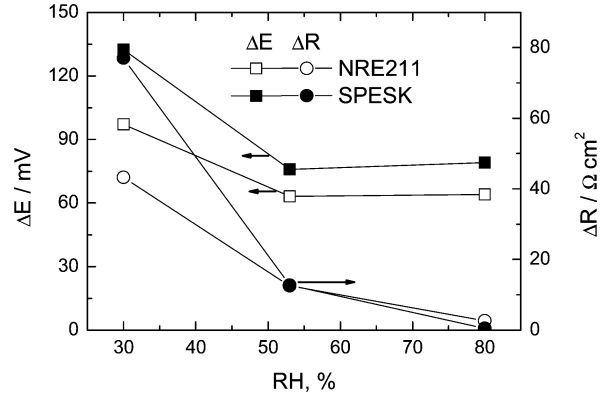

Figure 4. Differences in the cell voltage (ΔE) and the ohmic resistance (ΔR) between oxygen and air fuel cell operation at 0.4 A cm^{-2}.

Supporting Information Figure S1.[21] The fuel cell performance of the SPESK membrane was tested at 80 °C and compared with that of the Nafion NRE211 membrane (both membranes were 25 μm thick) in Figures 2 (H_2/O_2) and 3 (H_2/air). In both MEAs, Nafion was used as the binder in the catalyst layer (Nafion-GDE) so as to compare the differences of the membranes. The Nafion-GDE/SPESK MEA showed comparable $I-V$ performance to that of the Nafion-GDE/NRE 211 MEA at 53 and 80% RH. The ohmic resistance of SPESK was also comparable to that of Nafion NRE 211. The resistance was in good accordance with the value calculated from the in-plane proton conductivity in Supporting Information Figure S1. For example, the ohmic resistance at 53% RH in Figure 2 was ca. 50 mΩ cm^2, which corresponded to a proton conductivity of 0.05 S cm^{-1} for a 25 μm thick membrane. The proton conductivity under the same conditions was estimated to be 0.044 S cm^{-1} from Supporting Information Figure S1. The results imply that the resistance between membrane and electrodes was negligible and that the in-plane and through-plane proton conductivities were the same (isotropic proton conduction). Both MEAs showed similar fuel cell performance under H_2/O_2 and H_2/air operation at 53 and 80% RH (compare Figure 2 with Figure 3). However, the performance at 30% RH was lower with H_2/air than with H_2/O_2 for both MEAs. Since the fuel cells were operated at fixed gas utilization, the gas flow rate of air was five times faster than that of oxygen. The faster flow rate could deprive the cathode and membrane of water, causing a lower cell voltage and higher ohmic resistance.

Figure 4 shows differences in the cell voltage (ΔE) and the ohmic resistance (ΔR) of the two MEAs between oxygen and air conditions at 0.4 A cm^{-2} as a function of RH. The two MEAs showed comparable ΔR values above 53% RH, while the ΔR value was significantly higher for SPESK than for Nafion NRE 212 at 30% RH. The SPESK MEA showed higher ΔE values than those of the Nafion MEA at all RH conditions. The ΔE and ΔR values of the SPESK MEA at 30% RH were 132 mV and 77 mΩ cm^2, and those of the Nafion MEA were 97 mV and 43 mΩ cm^2, respectively. These results indicate that the performance of the electrodes might be different due to the nature of the membranes, even when the ohmic resistances (or the proton conductivities) of the membranes are equal (this issue is discussed below in connection with Figure 5). It is also noteworthy that the fuel cell performance of the SPESK MEA at 30% RH was superior compared to those of the other reported hydrocarbon ionomer membranes.[7,25−27]

To investigate the effect of the membrane thickness, fuel cells were operated with thicker SPESK and Nafion NRE212 membranes (50 μm thick). The results are shown in Supporting Information Figures S2 (H_2/O_2) and S3 (H_2/air). Similar to the thinner membrane, the thicker (50 μm) SPESK MEA showed comparable $I-V$ performance and ohmic resistance at 53 and 80% RH and lower $I-V$ performance and higher ohmic resistance at 20% RH in both H_2/O_2 and H_2/air operation, compared to those of the NRE 212 MEA. The large drop in the cell voltage for the thicker (50 μm) SPESK MEA at 20% RH could not be simply explained by a small increase in the ohmic resistance. The IR-free cell voltages for H_2/O_2 operation were compared between thin and thick membrane MEAs in Figure 5. The IR free cell voltages were nearly comparable over a wide range of current densities for the thin (25 μm) SPESK and NRE 211 membrane MEAs (Figure 5a), suggesting that the electrode performance was not affected by the membranes. In contrast, there were distinct differences in the IR-free cell voltages between the thick (50 μm) SPESK and NRE 212 membrane MEAs, especially at 20% RH and high current density (Figure 5b). A probable assumption is that the diffusion of water from

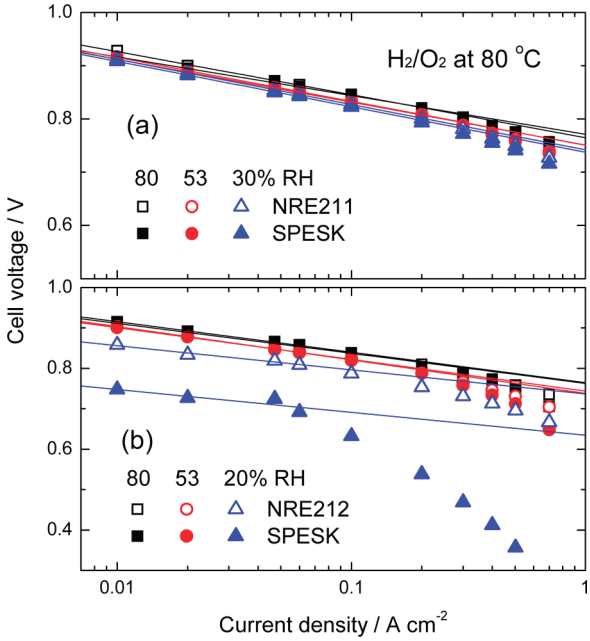

Figure 5. IR-free cell voltage of H_2/O_2 fuel cells with Nafion-GDE (a) 25 μm thick NRE 211 and SPESK MEAs and (b) 50 μm thick NRE 212 and SPESK MEAs at 80 °C.

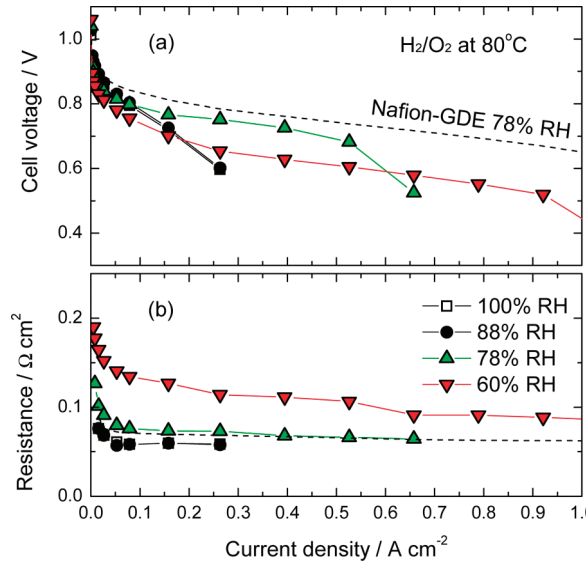

Figure 6. (a) Cell voltage and (b) ohmic resistance of an H_2/O_2 fuel cell with SPESK-GDE/NRE 212 MEA at 80 °C.

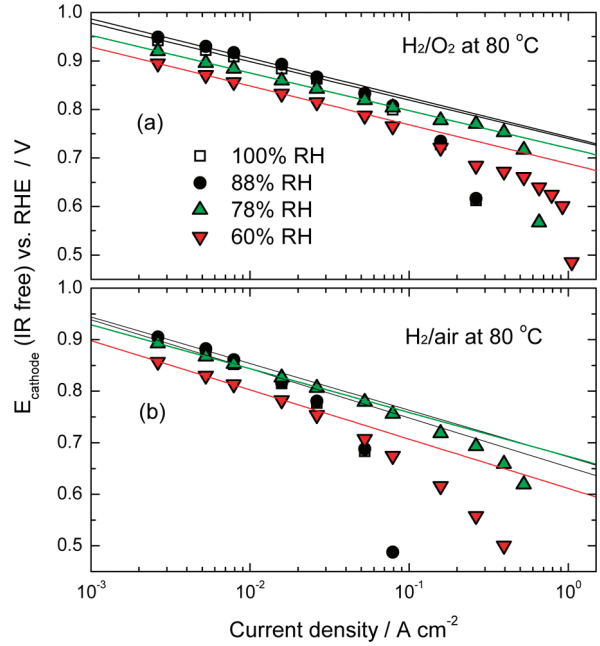

Figure 7. IR-free cathode potential of (a) H_2/O_2 and (b) H_2/air fuel cell with the SPESK-GDE/NRE 212 MEA at 80 °C.

the cathode to the anode (back-diffusion of water) was less in the thick SPESK membrane than that in Nafion NRE 212, and therefore the anode might have been starved for water, causing a higher overpotential under lower humidity conditions. The diffusion coefficient of water was estimated by the pulsed-field gradient NMR technique to be 2×10^{-11} m^2 s^{-1} for the SPESK membrane at 40 °C and 50% RH, which was 1 order of magnitude lower than that for the NRE 212 membrane (2×10^{-10} m^2 s^{-1}).[28] Similar results were obtained for a sulfonated poly(arylene sulfone) despite its very high IEC.[29] The higher ΔE of the SPESK MEA in Figure 4 can be reasonably explained by this assumption. A high flux of air at the cathode side could easily dry the cathode in the SPESK MEA. Therefore, the back-diffusion of water to the anode was insufficient causing a high ΔE even for the thin (25 μm) SPESK MEA but not as severe as thick (50 μm) SPESK MEA.

The hydrogen-limiting current density, which was calculated from linear sweep voltammograms, was much lower for the SPESK membrane than that for the Nafion NRE 212 membrane (Supporting Information Figure S4). The results coincide with the ex situ gas permeability measurement of the membranes.[22] The lower gas permeability is beneficial since the potential formation of hydrogen peroxide and the depression of the cathode potential would be mitigated.

Performance of SPESK-GDE/Nafion NRE 212 MEAs. In the above experiments, Nafion was used as the binder in the gas diffusion electrodes. To evaluate SPESK as the binder, we have prepared SPESK-GDE/NRE 212 MEAs, in which SPESK was used only as the cathode binder and Nafion was used as the anode binder and membrane (50 μm thick). Figure 6 shows the H_2/O_2 fuel cell performance and ohmic resistance of the SPESK-GDE/NRE 212 MEA at 80 °C. The maximum I−V performance was obtained at 78% RH and either higher or lower humidification caused lower performance. At 78% RH, however, the I−V performance of the SPESK-GDE/NRE 212 MEA was lower than that of the Nafion-GDE/NRE 212 MEA (dashed line), despite practically the same ohmic resistances. A similar tendency was observed in the H_2/air operation, as shown in Supporting Information Figure S5. The lower performance of the SPESK-GDE/NRE 212 MEA could be attributed to the cathode (SPESK-GDE), since the anodic overpotential was negligible when a Nafion membrane was used.[30] In Figure 7 are plotted IR-free cathode potentials of a fuel cell with the SPESK-GDE/NRE 212 MEA as a function of current density. At low current density, higher cathode potentials were obtained at higher humidity (88 and 100% RH). However, the cathode potentials became higher for 78% RH operation than those for 88 and 100% RH operation at higher current density.

To investigate the cathode performance in more detail, the mass activities (MA) of the Pt catalyst at 0.85 V, Tafel slopes, and current densities ($J_{\text{at } 0.75 \text{ V}}$) at 0.75 V (IR-free) were calculated for both H_2/O_2 and H_2/air conditions and plotted as a function of RH in Figure 8. MA is defined as the current at 0.85 V per unit Pt mass (A g_{Pt}^{-1}) and is a measure of the catalyst utilization. The MA values increased with increasing RH due to the improved proton conductivity. The MA values were lower

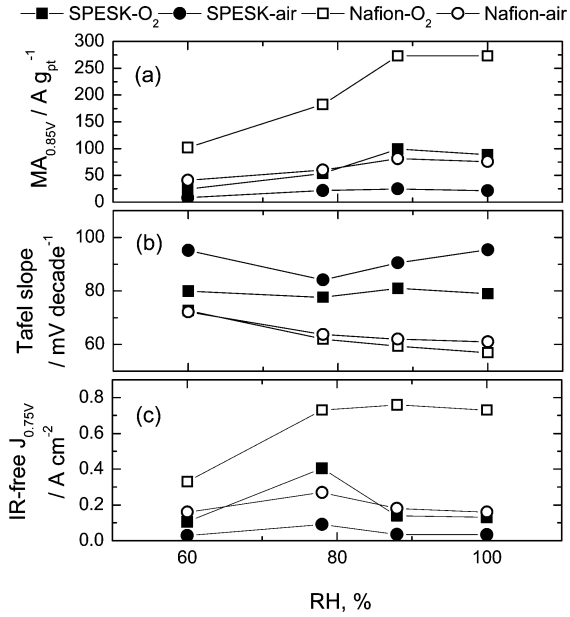

Figure 8. RH dependence of (a) mass activities (MA) at 0.85 V, (b) Tafel slopes, and (c) IR-free $J_{\text{at } 0.75 \text{ V}}$ of SPESK-GDE/NRE 212 and Nafion-GDE/NRE212 MEAs at 80 °C.

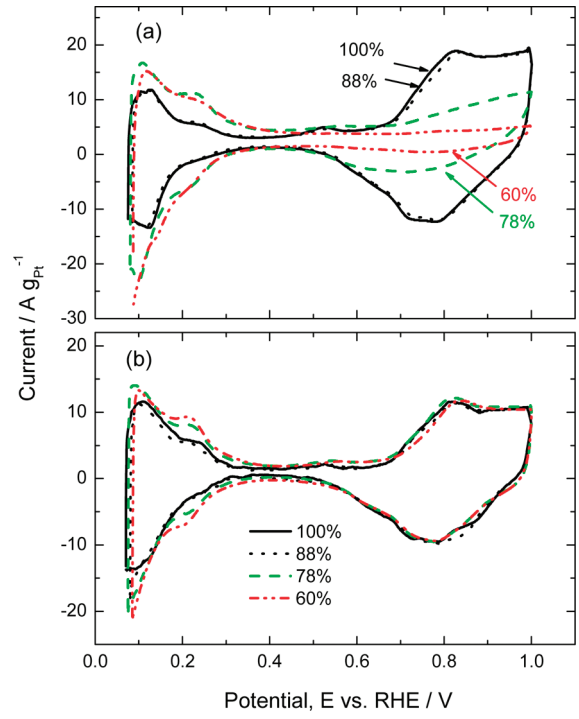

Figure 9. Cyclic voltammograms of (a) SPESK-GDE and (b) Nafion-GDE with NRE 212 membrane at 80 °C.

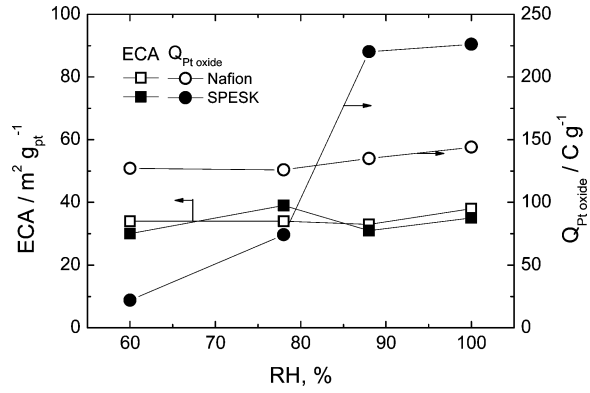

Figure 10. Humidity dependences of ECA and $Q_{\text{Pt oxide}}$ for the SPESK-GDE and Nafion-GDE at 80 °C.

for the SPESK-GDE than those for the Nafion-GDE, similar to our previous SPE ionomers.[30,31] The Tafel slopes for the SPESK-GDE were ca. −80 mV decade^{-1} with O_2 and −85 ∼ −95 mV decade^{-1} with air. These values were larger than the theoretical value (−70 mV decade^{-1}) for the kinetically controlled oxygen reduction reaction at 80 °C. Since the Tafel slopes were larger for the SPESK-GDE than those for the Nafion-GDE even at high RH (where the proton conductivities of SPESK and Nafion are comparable), the supply of O_2 and/or discharge of product water would have been insufficient. SPESK absorbs more water and swells more than Nafion (see Supporting Information Figure S1). The high swelling impedes efficient mass (O_2 and water) transport in the SPESK-GDE and causes such large Tafel slopes. The $J_{\text{at } 0.75 \text{ V}}$ value, which is the cathode potential for practical fuel cell operation, reflects the overall factors of Pt utilization, proton and mass transport. The $J_{\text{at } 0.75 \text{ V}}$ values showed a maximum at 78% RH for the SPESK-GDE with O_2 and air. Since the Pt utilization (or proton transport) and mass transport have opposite dependences on the humidity, the total performance of the GDE was balanced at intermediate humidity. In our previous report, we have demonstrated that the critical ionomer thickness of a sulfonated polyimide (SPI) ionomer covering the Pt/CB catalysts was 50 nm and the oxygen reduction reaction was controlled kinetically below this thickness at >0.7 V vs RHE.[32] The critical thickness of SPESK would be larger than that of SPI, taking the former's higher gas permeability into account. In a typical GDE, the ionomer thickness is on the order of several nanometers, and thus, diffusion of O_2 may not be the issue, but discharge of product water could be crucial.

Figure 9 shows CVs of the SPESK-GDE and Nafion-GDE at 80 °C and 60, 78, 88, and 100% RH. The electrochemically active surface areas (ECA) and the oxide formation charges ($Q_{\text{Pt oxide}}$)[33,34] were calculated from these CVs and are plotted as a function of RH in Figure 10. At 100% RH, the CV curve of the SPESK-GDE was very similar to that of the Nafion-GDE. The ECA and $Q_{\text{Pt oxide}}$ values were also comparable. The ECA values were roughly constant at any RH, while $Q_{\text{Pt oxide}}$ decreased with decreasing RH for both GDEs. The decrease in $Q_{\text{Pt oxide}}$ was much more significant for the SPESK-GDE. These results are in good accordance with the MA values of the SPESK-GDE and its dependence on RH in Figure 8. Similar results were obtained with our previous SPE of different chemical structure.[30] There were also some other reports on the lower cathode performances of hydrocarbon ionomer-GDEs than that of Nafion-GDE.[35,36] The lower values of $Q_{\text{Pt oxide}}$ imply that there were insufficient numbers of water molecules for the surface oxidation and/or the presence of specifically adsorbed molecules on the Pt surface. In the present case, the latter is likely to be dominant, since SPESK absorbs more water than Nafion over a wide range of humidity (see Supporting Information Figure S1). Possible adsorbates are anionic species such as sulfonate groups[31] and electron-rich groups such as aromatic rings.[37,38] The SPESK molecule contains both species in its chemical structure. Since Nafion does carry sulfonic acid groups but not aromatic rings, the aromatic rings of SPESK are the most probable adsorbates on Pt to impede the surface oxidation and oxygen reduction reactions.

Performance of SPESK-GDE/SPESK (all-SPESK) MEA. We have then prepared an SPESK-GDE/SPESK MEA (all-SPESK, Nafion-free MEA) and investigated the fuel cell

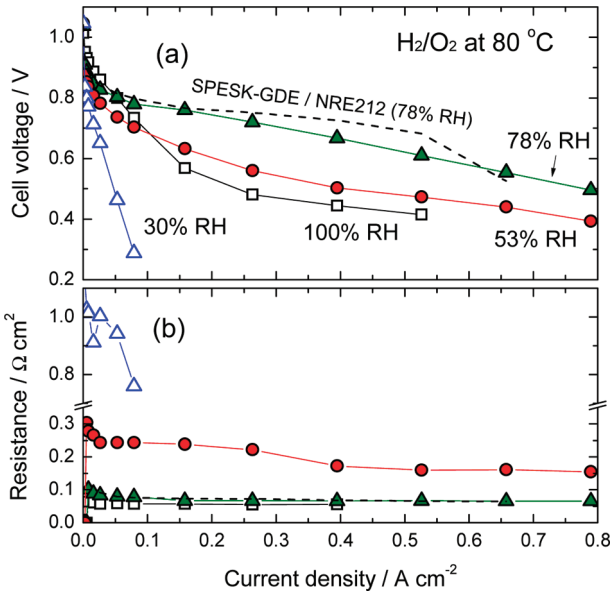

Figure 11. (a) Cell voltage and (b) ohmic resistance of an H_2/O_2 fuel cell with SPESK-GDE/SPESK MEA at 80 °C.

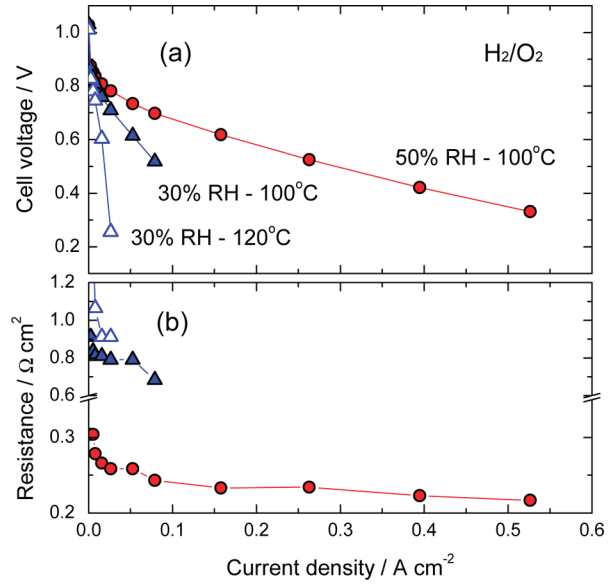

Figure 12. (a) Cell voltage and (b) ohmic resistance of an H_2/O_2 fuel cell with SPESK-GDE/SPESK MEA at 100 and 120 °C.

performance. Figure 11 shows the H_2/O_2 fuel cell performance and ohmic resistance of the SPESK-GDE/SPESK MEA at 80 °C. Similar to the results of the SPESK-GDE/Nafion MEA in Figure 6, the maximum performance was obtained at 78% RH. This tendency was the same for H_2/air operation (Supporting Information Figure S6). The fuel cell was also operated under more severe conditions (100 °C and 30% or 50% RH, and 120 °C and 30% RH, Figure 12 and Supporting Information Figure S7). At 100 °C and 50% RH, the fuel cell could be operated up to a current density of 0.5 A cm^{-2} with reasonable ohmic resistance (220 mΩ cm^2). The ohmic resistance was somewhat higher than that calculated from the proton conductivity of the SPESK membrane (125 mΩ cm^2 at 110 °C). In addition, because of the high overpotential both at the cathode (derived from the specific adsorption) and the anode (caused by the low flux of water from the cathode), the cell voltage dropped significantly with increasing current density. The fuel cell performance was even worse at lower RH and higher temperature. The results suggest that high water transport capability and low adsorbability of ionomers on the catalysts are crucial requirements for alternative ionomer materials, especially for fuel cells operable at high temperature and low humidity.

Conclusions

The SPESK block copolymer membrane with IEC = 1.8 mequiv g^{-1} showed comparable fuel cell performance to that for a Nafion membrane at 80 °C and 30% RH. While the performance was very promising in terms of alternative, hydrocarbon-based ionomers being used as membranes, the membrane thickness needs to be taken into account, since insufficient water flux thorough the membrane can increase the overpotential at the anode. The SPESK did not function very well as the cathode binder regardless of the temperature and the humidity. The aromatic rings and/or the sulfonic acid groups of the SPESK appeared to be adsorbed on the platinum catalyst, which lowered the cathode performance (oxygen reduction reaction activity). The results of this study have provided us with important insights for designing alternative ionomer materials to be used as the binder in the gas diffusion electrodes; high water transport capability and decreased specific adsorbability on the catalyst should be taken more into account.

Acknowledgment. This work was partly supported by the New Energy and Industrial Technology Development Organization (NEDO) through the Research on Nanotechnology for High Performance Fuel Cells (HiPer-FC) Project, and the Ministry of Education, Culture, Sports, Science, and Technology (MEXT) of Japan through a Grant-in-Aid for Scientific Research (20350086). We thank Drs. Koh Kidena, Takahiro Ohkubo, and Akihiro Ohira of FC-Cubic, Japan for the measurement of the diffusion coefficient of water by pulsed-field gradient NMR.

Supporting Information Available: RH dependence of proton conductivity, fuel cell performance, and CV data. This material is available free of charge via the Internet at http://pubs.acs.org.

References and Notes

(1) Lafitte, B.; Karlsson, L. E.; Jannasch, P. *Macromol. Rapid Commun.* **2002**, *23*, 896–900.
(2) Wang, F.; Hickner, M.; Kim, Y. S.; Zawodzinski, T. A.; McGrath, J. E. *J. Membr. Sci.* **2002**, *197*, 231–242.
(3) Chikashige, Y.; Chikyu, Y.; Miyatake, K.; Watanabe, M. *Macromolecules* **2005**, *38*, 7121–7126.
(4) Xing, P.; Robertson, G. P.; Guiver, M. D.; Mikhailenko, S. D.; Wang, K.; Kaliaguine, S. *J. Membr. Sci.* **2004**, *229*, 95–106.
(5) Gil, M.; Ji, X.; Li, X.; Na, H.; Hampsey, J. E.; Lu, Y. *J. Membr. Sci.* **2004**, *234*, 75–81.
(6) Shang, X.; Tian, S.; Kong, L.; Meng, Y. *J. Membr. Sci.* **2005**, *266*, 94–101.
(7) Zhu, Z.; Walsby, N. M.; Colquhoun, H. M.; Thompsett, D.; Petrucco, E. *Fuel Cells* **2009**, *9*, 305–317.
(8) Miyatake, K.; Zhou, H.; Matsuo, T.; Uchida, H.; Watanabe, M. *Macromolecules* **2004**, *37*, 4961–4966.
(9) Yin, Y.; Suto, Y.; Sakabe, T.; Chen, S.; Hayashi, S.; Mishima, T.; Yamada, O.; Tanaka, K.; Kita, H.; Okamoto, K.-i. *Macromolecules* **2006**, *39*, 1189–1198.
(10) Gao, Y.; Robertson, G. P.; Kim, D.-S.; Guiver, M. D.; Mikhailenko, S. D.; Li, X.; Kaliaguine, S. *Macromolecules* **2007**, *40*, 1512–1520.
(11) Wainright, J. S.; Wang, J.-T.; Weng, D.; Savinell, R. F.; Litt, M. *J. Electrochem. Soc.* **1995**, *142*, L121–L123.
(12) Jones, D. J.; Roziere, J. *J. Membr. Sci.* **2001**, *185*, 41–58.
(13) Fujimoto, C. H.; Hickner, M. A.; Cornelius, C. J.; Loy, D. A. *Macromolecules* **2005**, *38*, 5010–5016.
(14) Goto, K.; Rozhanskii, I.; Yamakawa, Y.; Otsuki, T.; Naito, Y. *Polym. J.* **2009**, *41*, 95–104.
(15) Takimoto, N.; Wu, L.; Ohira, A.; Takeoka, Y.; Rikukawa, M. *Polymer* **2009**, *50*, 534–540.

(16) Fuel Cell Program's Multi-Year Research, Development, and Demonstration Plan. http://www1.eere.energy.gov/hydrogenandfuelcells/fuelcells/fc_challenges.html (accessed June 1, 2009).
(17) Miyatake, K.; Chikashige, Y.; Higuchi, E.; Watanabe, M. *J. Am. Chem. Soc.* **2007**, *129*, 3879–3887.
(18) Roy, A.; Yu, X.; Dunn, S.; McGrath, J. E. *J. Membr. Sci.* **2009**, *327*, 118–124.
(19) Matsumura, S.; Hlil, A. R.; Lepiller, C.; Gaudet, J.; Guay, D.; Shi, Z.; Holdcroft, S.; Hay, A. S. *Macromolecules* **2008**, *41*, 281–284.
(20) Bae, B.; Miyatake, K.; Watanabe, M. *ACS Appl. Mater. Interfaces* **2009**, *1*, 1279.
(21) Bae, B.; Yoda, T.; Miyatake, K.; Uchida, H.; Watanabe, M. *Angew. Chem., Int. Ed.* **2010**, *49*, 317–320.
(22) Bae, B.; Miyatake, K.; Watanabe, M. *Macromolecules* **2010**, *43*, 2684–2691.
(23) Watanabe, M.; Motoo, S. *J. Electroanal. Chem.* **1975**, *60*, 259–266.
(24) Watanabe, M.; Motoo, S. *J. Electroanal. Chem.* **1975**, *60*, 275–283.
(25) Asano, N.; Aoki, M.; Suzuki, S.; Miyatake, K.; Uchida, H.; Watanabe, M. *J. Am. Chem. Soc.* **2006**, *128*, 1762–1769.
(26) Wiles, K. B.; de Diego, C. M.; de Abajo, J.; McGrath, J. E. *J. Membr. Sci.* **2007**, *294*, 22–29.
(27) Tian, S.; Meng, Y.; Hay, A. S. *Macromolecules* **2009**, *42*, 1153–1160.
(28) Kidena, K.; Ohkubo, T.; Takimoto, N.; Ohira, A. *Eur. Polym. J.* **2010**, *46*, 450–455.
(29) Araujo, C. C. d.; Kreuer, K. D.; Schuster, M.; Portale, G.; Mendil-Jakani, H.; Gebel, G.; Maier, J. *Phys. Chem. Chem. Phys.* **2009**, *11*, 3305–3312.
(30) Yoda, T.; Shimura, T.; Bae, B.; Miyatake, K.; Uchida, M.; Uchida, H.; Watanabe, M. *Electrochim. Acta* **2009**, *54*, 4328–4333.
(31) Kabasawa, A.; Uchida, H.; Watanabe, M. *Electrochem. Solid-State Lett.* **2008**, *11*, B190–B192.
(32) Miyatake, K.; Omata, T.; Tryk, D. A.; Uchida, H.; Watanabe, M. *J. Phys. Chem. C* **2009**, *113*, 7772–7778.
(33) Gnanamuthu, D. S.; Petrocelli, J. V. *J. Electrochem. Soc.* **1967**, *114*, 1036–1041.
(34) Vogel, W. M.; Baris, J. M. *Electrochim. Acta* **1977**, *22*, 1259–1263.
(35) Ramani, V.; Swier, S.; Shaw, M. T.; Weiss, R. A.; Kunz, H. R.; Fenton, J. M. *J. Electrochem. Soc.* **2008**, *155*, B532–B537.
(36) Astill, T.; Xie, Z.; Shi, Z.; Navessin, T.; Holdcroft, S. *J. Electrochem. Soc.* **2009**, *156*, B499–B508.
(37) Moore, J. M.; Adcock, P. L.; Lakeman, J. B.; Mepsted, G. O. *J. Power Sources* **2000**, *85*, 254–260.
(38) Li, H.; Zhang, J.; Fatih, K.; Wang, Z.; Tang, Y.; Shi, Z.; Wu, S.; Song, D.; Zhang, J.; Jia, N.; Wessel, S.; Abouatallah, R.; Joos, N. *J. Power Sources* **2008**, *185*, 272–279.

JP1052908